

Kinetic-energy distribution of excited atoms produced when H_2 and D_2 molecules are dissociated by electron impact

G. N. Polyakova, A. I. Ranyuk, and V. F. Erko

Physicotechnical Institute, Ukrainian Academy of Sciences
(Submitted July 14, 1977)
Zh. Eksp. Teor. Fiz. 73, 2131-2141 (December 1977)

The kinetic-energy distributions are investigated of excited hydrogen and deuterium atoms in states with principal quantum numbers $n = 3, 4, 5$, and 6, produced in the dissociation of H_2 and D_2 molecules by electron impact with energy 90-300 eV. It is shown that the dissociative excitation of the H_2 and D_2 molecules results in two groups of atoms, slow and fast. The relative number of the slow and fast atoms depends on the principal quantum number and on the molecule mass. The dependence on the molecule mass points to an important role of the predissociation process in the formation of the group of slow fragments.

PACS numbers: 34.80.Gs

Information on the kinetic energies of hydrogen atoms in states with principal quantum numbers $n \geq 3$ produced by dissociation of hydrogen molecules, is very skimpy. The reason is that the time-of-flight procedure, which is widely used to measure the kinetic-energy distributions, cannot be applied to atoms in states with short lifetimes. Information on the kinetic energies can be obtained for such atoms from the Doppler broadening of the spectral lines, and this calls for measurement of the intensity distribution in the contours of these lines. Such a procedure was used in^[1,2], and the results have shown that the dissociation of molecular hydrogen gives rise to two groups of excited atoms, slow and fast; this agrees with the estimates given in a preceding paper.^[3] The method used in^[2] to reduce the contours of the spectral lines has made it possible to extract from them more detailed information in the velocity distributions of the excited hydrogen atoms.

According to the hypotheses advanced in^[1,2], one of the possible processes whereby slow excited atoms are produced may be the predissociation of the Rydberg states of the hydrogen molecule, converging to the ground state of the molecular ion. The probability of this process depends on the reduced mass of the molecule. Therefore information on the kinetic-energy distributions of the excited deuterium atoms may be useful in the assessment of the relative role of the predissociation process in the formation of the slow excited atoms. In the present study, we measured the intensity distributions in the contours of the Balmer-line series excited by dissociation of deuterium molecules by electron impact. In addition, we repeated the measurements of the contours of the spectral lines of hydrogen atoms in states with principal quantum numbers $n = 3, 4$, and 5 and performed new measurements for hydrogen atoms in the state with $n = 6$. Compared with our previous paper,^[2] we take into account here, besides the instrumental broadening of the spectral lines, also other possible broadening mechanisms, and this has enabled us to obtain the kinetic-energy distributions in the low-energy region. The kinetic-energy distributions for excited hydrogen and deuterium atoms were obtained from the experimental distributions of the intensities by the mathematical-reduction procedure described in^[2].

MEASUREMENT PROCEDURE AND REDUCTION OF RESULTS

The setup used for the measurements is described in^[2]. The intensity distribution in the contours of the spectral lines was measured by pressures $(2-7) \times 10^{-3}$ Torr. Investigations of these distributions for hydrogen^[2] have shown that in this pressure range the intensity distributions do not depend on the pressure. Measurements of the dependences of the Balmer-series line intensities on the pressure have shown that the 2×10^{-3} Torr pressure is in the single collision region. The intensity distributions in the line contours were measured with a scanning Fabry-Perot interferometer placed past the large-aperture MDR-2 monochromator. The intensities were recorded photoelectrically.

Information on the kinetic energies of the atoms can be obtained from the spectral-line contours if the broadening due to the Doppler effect is predominant. It is therefore necessary to exclude all effects that cause additional line broadening. For lines of the Balmer series these effects can be: 1) instrumental broadening; 2) broadening due to the Stark and Zeeman effects; 3) broadening due to the fact that each Balmer-series line is complex because of the tight proximity of the fine-structure levels; 4) broadening due to thermal motion of the parent molecule.

The line broadening due to the effect 1 was taken into account in the following manner: the measured intensity distribution $f(\lambda')$ is connected with the true distribution $\varphi(\lambda)$ by the relation

$$f(\lambda') = \int_{-\infty}^{\infty} a(\lambda, \lambda') \varphi(\lambda) d\lambda. \quad (1)$$

The function $a(\lambda, \lambda')$, which describes the instrumental line broadening, was determined with the aid of the mercury lines closest to lines α , β , γ , and δ . Equation (1) was solved by the method of statistical regularization.

The broadening due to effect 2 was estimated in^[1], where it was found to be negligibly small. In our case there was no collimating magnetic field in the collision chamber. In addition, the electron-beam density was

$\sim 4 \text{ mA/cm}^2$, i.e., lower than in^[11]. Therefore the role of effect 2 was even smaller under the conditions of our experiment.

The broadening due to effect 3 could be taken into account by resolving the measured line contour into components. This was done by us for the lines H_α and D_α . These lines are complex and consist of seven components corresponding to the transitions

$$3^2D_{5/2} \rightarrow 2^2P_{3/2}, \quad 3^2D_{3/2} \rightarrow 2^2P_{1/2}, \quad 3^2S_{1/2} \rightarrow 2^2P_{3/2}, \quad 3^2D_{5/2} \rightarrow 2^2P_{1/2}, \\ 3^2S_{3/2} \rightarrow 2^2P_{3/2}, \quad 3^2P_{3/2} \rightarrow 2^2S_{1/2}, \quad 3^2P_{1/2} \rightarrow 2^2S_{1/2}.$$

It is known^[4,5] that in the case of dissociative excitation of a line by electron impact the state $3p$ has negligibly small excitation cross sections compared with the states $3s$ and $3d$. In addition, the excitation cross sections of the state $3s$ are $\sim 30\%$ of the total excitation cross section of the H_α line. According to the transition probabilities, the intensity of the $3^2S_{1/2} \rightarrow 2^2P_{3/2}$ component should be twice as large as the intensity of the component $3^2S_{1/2} \rightarrow 2^2P_{1/2}$. We used these data and the known spacings between the fine-structure components to resolve the measured intensity contours of the H_α and D_α lines. Since the spacing between the $3^2D_{5/2} \rightarrow 2^2P_{3/2}$ and $3^2D_{3/2} \rightarrow 2^2P_{3/2}$ components is 0.015 \AA , we regarded these components as superimposed.

To resolve the H_α and D_α line contours, the intensity distributions were measured with maximum attainable resolution of the interferometer, at which the overlap of neighboring interference orders could be neglected. We used for these measurements a Fabry-Perot interferometers with distance 3 mm between mirrors, thus ensuring a resolution $\sim 10^5$. From the distributions obtained in this manner we determined the broadening due to the apparatus. The function $a(\lambda, \lambda')$ was determined in this case with the aid of the lines of an helium-neon laser of wavelength $\lambda = 6328 \text{ \AA}$. The intensity distributions obtained in this manner for the H_α and D_α lines excited by dissociation of the molecules H_2 and D_2 by 300-eV electrons. The figure shows also the resolution of each of the H_α and D_α contours into four contours corresponding to the transitions from the $3s$ and $3d$ levels to the $3p$ levels. The resolution was effected in such a way that the intensity distribution in all four components

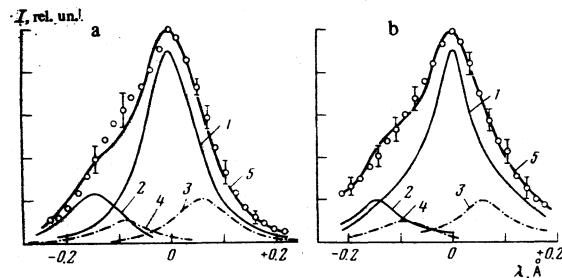


FIG. 1. Intensity distributions in the line contours: a— H_α ; b— D_α ; points—experimental distributions with instrumental distortion eliminated. The half-widths of the instrumental function for H_α and D_α are 0.07 and 0.05 \AA . Curves—resolution of the contour into components: 1— $3^2D_{5/2,3/2} \rightarrow 2^2P_{3/2}$; transition; 2— $3^2D_{3/2} \rightarrow 2^2P_{1/2}$; 3— $3^2S_{1/2} \rightarrow 2^2P_{3/2}$; 4— $3^2S_{1/2} \rightarrow 2^2P_{1/2}$; 5—sum of curves 1–4.

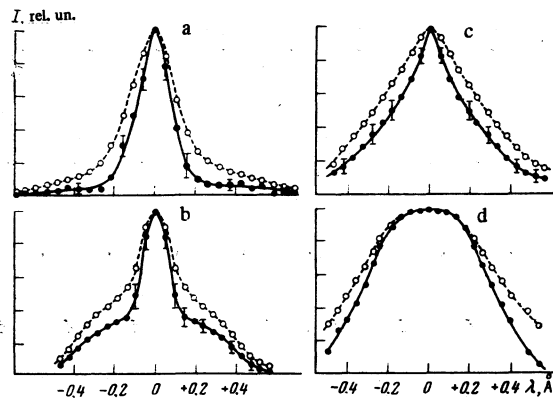


FIG. 2. Intensity distribution in line contours: a— D_α , b— D_β , c— D_γ , d— D_δ . Light points and dashed curve—experimental distribution, dark points and solid curve—distribution with the instrumental distortion excluded.

be described by the same function. As seen from Fig. 1, the measured line contour (with allowance for the correction for the instrumental broadening) agrees quite well with a contour that constitutes a sum of the four contours shown in this figure.

We were unable to perform the measurements for lines β and γ at high resolution and determine their broadening as a result of effect 3, since these lines were broader than line α (see Fig. 2).

The line broadening due to the effect 4 was taken into account in the following manner. In the case of dissociative excitation, the intensity distribution in the contour of the spectral line $\varphi(\lambda)$ or $\varphi(V_x)$ (V_x is the projection of the velocity on the observation axis) is connected with the distribution of the radiating atoms in the velocities $P(v)$ by the relation^[6]

$$\varphi(V_x) = \int_{v_x-\tau}^{v_x+\tau} \int_{v_y-\tau}^{v_y+\tau} R_x(V_x - C_x, v) T(C_x) P(v) dC_x dv, \quad (2)$$

where $T(C_x)$ is the Maxwellian velocity distribution for the parent molecule AB:

$$T(C_x) dC_x = \frac{1}{\alpha \sqrt{\pi}} \exp\left(-\frac{C_x^2}{\alpha^2}\right) dC_x;$$

$\alpha = [2kT/(m_A + m_B)]^{1/2}$ is the most probable thermal velocity of the molecule AB, and R_x is a factor that takes into account the angular distribution of the atoms that move apart as a result of the dissociation process. This factor, in the case of dissociative excitation, depends on the type of the transition between the states of the molecule and on the electron energy. Zare^[7] calculated the angular distributions of the protons produced in the dissociation of the H_2^+ molecule by electron impact. According to these calculations the degree of anisotropy in the angular distribution was maximal at the threshold of proton production, and then decreased with increasing electron energy. For electron energies from 100 to 300 eV, the proton angular distributions were isotropic. Indeed, Dunn, Kieffer, and Van Brunt^[8,9] observed such a dependence of the degree of anisotropy for protons produced in the course of dissociative ionization of hydrogen

molecules by electron impact. Since we used electrons with energies 90, 130, and 300 eV, the angular distribution could be regarded as isotropic. In this case $R_x = 1/v$.^[6] At low velocities of the excited atoms $v < 2\alpha$ ($E < 0.05$ eV),¹⁾ the broadening due to effect 4 was taken into account by solving Eq. (2) in two stages: we first determined the derivative $d\varphi(V_x)/dV_x$, and then used the method of statistical regularization to solve an integral equation with a kernel in the form

$$\exp[-(V_x+v)^2/\alpha^2] - \exp[-(V_x-v)^2/\alpha^2].$$

At sufficiently high velocities of the excited atoms, $v > 2\alpha$, the translational motion of the parent molecule does not influence the shape of the line contour; in this case the velocity distributions $P(v)$ can be obtained for isotropic angular distributions from the simpler relation

$$\varphi(V_x) = \int_{v_1}^{\infty} \frac{1}{v} P(v) dv. \quad (3)$$

Thus, for $v > 2\alpha$ the velocity distributions $P(v)$, and subsequently also the kinetic-energy distributions $P(E)$, were obtained by solving Eq. (3). This equation was solved also by the regularization method. An essential factor in this study was an estimate of the error in the final result—in the distribution $P(E)$ in the kinetic energies of the excited particles, inasmuch as in this case the error includes not only the experimental error but also the error due to the mathematical reduction of the measured intensity distributions. The last error, in turn, depends on the errors of the initial information. To obtain stable and reproducible solutions of the integral equations (1)–(3) it was therefore necessary to decrease the errors in the initial function $f(\lambda')$. To this end we usually recorded for each contour no less than 30–50 interference rings. The instrumental broadening function $a(\lambda, \lambda')$ was measured separately for each run.

Within the limits of the measurement error, the functions $f(\lambda')$ turned out to be the same at electron energies 90, 130, and 300 eV for all the measured Balmer lines of hydrogen and deuterium. To reduce the errors we therefore averaged for these energies the functions $\varphi(\lambda)$ which were, on the one hand, the solutions of Eq. (1), and on the other, the initial functions for Eqs. (2) or (3).

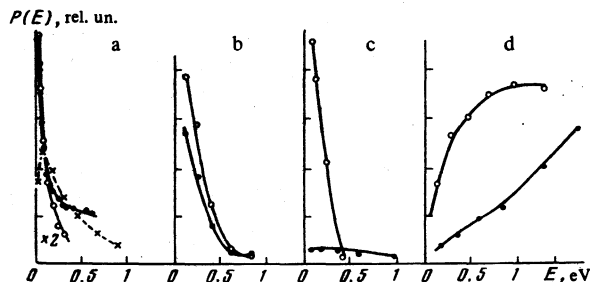


FIG. 3. Kinetic-energy distributions for slow excited atoms: a—distributions calculated from the Doppler broadening for the individual line components: \circ — H_α , \bullet — D_α , \times —calculation for the unresolved D_α line; b ($n=4$), c ($n=5$), d ($n=6$), \circ —hydrogen atoms, \bullet —deuterium atoms. The distributions were calculated from the Doppler broadening of the unresolved lines.

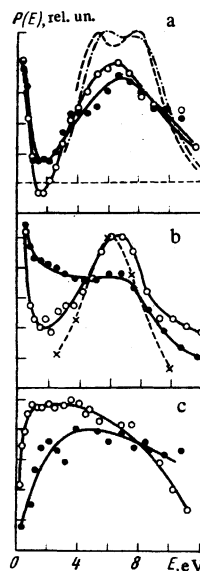


FIG. 4. Kinetic energy distributions for fast excited hydrogen (\circ) and deuterium (\bullet) atoms in the states $n=4$ (a), $n=5$ (b), and $n=6$ (c). Dash-dot curve—distribution for H^+ ions^[8]; dashed—distribution for D^+ ions^[8]; \times and dashed curve—distribution for hydrogen atoms in states with $n \geq 15$.^[11] (The dashed curves are shifted along the abscissa axis.)

To find the final error of the function $P(E)$ we performed the measurements for a number of lines at various resolving powers of the apparatus.²⁾ For the H_α and D_α lines, the measurements were made in cases when the half-width of the instrumental function $a(\lambda, \lambda')$ was 0.06 and 0.16 Å; its value for β and γ was 0.12 and 0.25 Å. We next compared the $P(E)$ functions calculated for the experimental data obtained at various resolving powers of the apparatus. This comparison has shown that the error in the determination of the function $P(E)$ amounts to ≈ 20 – 25% . This agrees approximately with the error estimates made in^{[2], 3)}

MEASUREMENT RESULTS AND DISCUSSION

Figure 2 shows the measured contours of the lines D_α , D_β , D_γ , and D_δ as well as the contours corrected for the instrumental broadening. The half-widths of the instrumental function for these lines were respectively of the order of 0.16, 0.12, 0.13, and 0.22 Å. It turned out that, just as for the hydrogen atoms, two groups of excited deuterium atoms are observed—slow and fast. Figures 3 and 4 show the kinetic-energy distributions for these two groups of atoms.⁴⁾ It is seen from the figures that the distributions $P(E)$ depend on the molecule mass and on the principal quantum number n .

Figure 3a shows the function $P(E)$ calculated for the intensity distributions in an individual fine-structure component and for the unresolved contour of the D_α line. As seen from the figure, for energies $E > 0.1$ eV these distributions differ little, and at $E < 0.1$ eV the functions $P(E)$ calculated for an individual component have a qualitatively different behavior on the low-energy side. A similar pattern was observed also for the H_α line (Fig. 3a shows only the $P(E)$ distribution calculated for an individual component of the H_α line). Thus, allowance for the fine structure of the lines H_α and D_α has made it possible to refine the form of the function $P(E)$ in the low-energy region.

For energies $E < 0.05$ eV, in the case of the H_α and

D_α lines, account was taken also of the contribution of the thermal motion of the parent molecule to the distribution in the kinetic energies. Figure 5 shows the $P(E)$ distributions obtained by solving Eq. (2). Allowance for this effect determined the behavior of the function $P(E)$ in the energy region $E < 0.05$ eV.

For the lines β , γ , and δ the measurements were made with the contours unresolved. Therefore the results for the states with $n=4, 5$, and 6 are shown in Fig. 3 for energies $E > 0.1$ eV.

SLOW ATOMS

Slow excited atoms of hydrogen and deuterium can be produced by two processes. The first is the Franck-Condon transition of the molecule from its ground state to the repulsion branches of the bound molecular states having as the dissociation limit a hydrogen (or deuterium) atom in the ground state and a hydrogen (deuterium) atom in a state with $n \geq 3$. This process was observed in the case of production of highly excited metastable hydrogen atom following dissociation of hydrogen molecules by electron impact.^[11] The second process that leads to the appearance of slow atoms may be the transition of a molecule to higher Rydberg states that converge to the ground state of the molecular ion, followed by pre-dissociation of the state into a lower-lying state whose dissociation limit is a hydrogen (deuterium) atom in the ground state and a hydrogen (deuterium) atom in a state with $n \geq 3$. This process was observed experimentally in the case of electron impact for hydrogen atoms in a state with $n=2$,^[12] and in the case of photoabsorption for hydrogen and deuterium atoms with $n \geq 3$.^[13] The theoretical calculations for the rates of the aforementioned dissociation process are given in a paper by Berry and Nielsen.^[14]

A competing channel for the decay of the Rydberg states of the H_2 and D_2 molecules can be autoionization into the ground state of the corresponding molecular ion. According to the estimates of Berry and Nielsen, the pre-dissociation rates has higher rates for transitions with minimal change of the principal quantum number⁵⁾ Δn of the Rydberg states. Autoionization has the highest rates for a minimal change Δv of the vibrational quantum number. Because of these circumstances, the lower terms of the Rydberg series decay predominantly via predissociation, while the higher ones decay via autoionization.

Using the calculations of Berry and Nielsen,^[14] we estimated the summary predissociation and autoioniza-

tion rates for on Rydberg series ($n'p\sigma$). For the terms of this series with $n' > 6$ we estimated the rates of pre-dissociation with formation of atoms in states $n \geq 4$. In the estimates we used data for the pre-dissociation rates of states that lead to the appearance of states with $n=3$, and assumed the pre-dissociation rate to be proportional to $(n')^{-3}$. Table I lists the results of these estimates. The calculations of Berry and Nielsen were made for Rydberg levels in a state with rotational quantum number $K=0$. Their calculations of the pre-dissociation and autoionization rates for higher K have shown that these rates hardly depend on K . In a number of cases shown in the table, the pre-dissociation of Rydberg states with $K=0$ was unable, from energy consideration to cause the appearance of excited atoms with a chosen value of n . However, such a pre-dissociation become possible already at $K=1$. In this case we estimated the pre-dissociation and autoionization rates from the data of Berry and Nielsen for the Rydberg states with $K=0$.

The measurements described here and the method of their reduction make it possible to compare the obtained data with the theoretical calculations of^[14]. As seen from Fig. 3, the number of deuterium atoms in states with $n=3$ and $n=4$ differs insignificantly from the number of the hydrogen atoms in the same state. A possible explanation is that the hydrogen and deuterium atoms stem in this case from Rydberg states that decay predominantly via predissociation (see the table). However, the number of deuterium atoms is much less than the number of hydrogen atom already for the state with $n=5$. The reason is that the hydrogen atoms in the state with $n=5$ can stem from the $8p\sigma$ state, for which the decay channel via predissociation is predominant. On the other hand in the case of the D_2 molecules the Rydberg states that can serve as a source of deuterium atoms in a state with $n=5$, decay predominantly via autoionization. For the H_2 molecule this case occurs probably for Rydberg states that are the sources of hydrogen atoms in a state with $n=6$ (see the table). This explains the change in the form of the $P(E)$ curve for hydrogen atoms with $n=6$ compared with those for $n=3, 4$, and 5 . Thus, comparison of our measurements with the theoretical calculations has demonstrated the important role of the pre-dissociation process in the formation of slow excited hydrogen and deuterium atoms. For the predissociation process, the number of excited atoms will decrease as their kinetic energy decreases to zero. For example, predissociation of the state $6p\sigma$ with formation of hydrogen in a state with $n=3$ is energywise possible for a vibrational level $v \geq 7$. The state $v=6$ can be a source of hydrogen atoms with $n=3$ at large values of the rotational quantum number. High rotational levels of the molecule are populated at room temperature insignificantly in comparison with the zeroth and first levels. However, as follows from Fig. 5, when the kinetic energy E approaches zero, the function $P(E)$ increases. This growth can be attributed to the contribution of the first dissociation process to the formation of the slow excited atoms, namely, the transition to the repulsion branches of the bound molecular states. Ford and Docken^[15] calculated the $P(E)$ distributions for protons produced as a result of the transition from the ground state

TABLE I.

Transition	Rate of pre-dissociation of upper state, sec ⁻¹	Rate of autoionization of upper state, sec ⁻¹	end product of the pre-dissociation
$6p\sigma \rightarrow 5p\sigma$ ($v=7-14, K=0$)	$4.3 \cdot 10^{13}$	$3.5 \cdot 10^{10}$	H ($n=3$)
$7p\sigma \rightarrow 6p\sigma$ ($v=11-14, K=0$)	$8.1 \cdot 10^{12}$	$1.6 \cdot 10^{11}$	H ($n=4$)
$8p\sigma \rightarrow 7p\sigma$ ($v=14, K=1$)	$1.6 \cdot 10^{12}$	$1 \cdot 10^{11}$	H ($n=5$)
$12p\sigma \rightarrow 8p\sigma$ ($v=14, K=1$)	$1.6 \cdot 10^9$	$2.4 \cdot 10^{11}$	H ($n=6$)
$6p\sigma \rightarrow 5p\sigma$ ($v=11-14, K=0$)	$6 \cdot 10^{12}$	10^8	D ($n=3$)
$8p\sigma \rightarrow 6p\sigma$ ($v=14, K=1$)	$2.5 \cdot 10^{10}$	$2 \cdot 10^8$	D ($n=4$)

Note: v -vibrational quantum number of upper state, K -rotational quantum number.

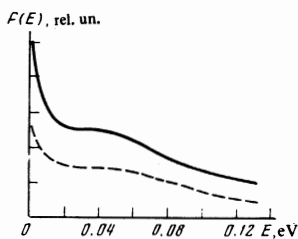


FIG. 5. Kinetic-energy distributions of hydrogen atoms (solid curve) and deuterium atoms (dashed) in a state with $n=3$ at kinetic energies $E < 0.1$ eV.

of the H_2 molecule to the repulsion branch of the molecular ion H_2^+ . In this case the function $P(E)$ had a maximum value at $E=0$ and decreased towards higher values of E . The repulsion branches of the Rydberg-state potential curves are almost parallel to the repulsion branch of the potential curve for the molecular ion H_2^+ (D_2^+). Consequently, the form of the function $P(E)$ for the excited atoms produced as a result of the first process will be the same as for protons; this explains the behavior of the function $P(E)$ at very small values of E (Fig. 5).

FAST ATOMS

The $P(E)$ distribution for fast excited hydrogen and deuterium atoms in states with $n=4, 5$, and 6 are shown in Fig. 2. For the state with $n=3$, the relative number of fast atoms is small (Fig. 3). It was therefore impossible to obtain reliable and reproducible results for the $P(E)$ distribution of fast atoms.

Since the dissociation of H_2 and D_2 molecules with formation of excited fragments in states with $n \geq 4$ comes from Rydberg states of the molecules, an attempt can be made to employ the "ion-core" model to describe the dissociation process. The previous measurements of the distributions $P(E)$ for highly excited atoms produced upon dissociation of O_2 , N_2 , and CO molecules^[16-18] have shown that this model can be used to describe the dissociative excitation process. According to the "ion-core" model, the appearance potentials and the kinetic energies of the atoms produced in the decay of Rydberg states approximately equal those for the ions produced in dissociative ionization. Figure 4a shows the $P(E)$ distributions for the ions H^+ and D^+ produced by dissociative ionization of H_2 and D_2 molecules by 290-eV electrons.^[8] As seen from Fig. 4a, the $P(E)$ distributions for the ions and excited atoms have approximately the same form. In addition, the measured appearance potentials of the excited fast atoms^[11] are located at ~ 26 eV, and this value, with allowance for the inaccuracy of its measurement, is close enough to the potential 28 eV of the appearance of ions with energy 8 eV at the distribution maximum. This group of H^+ and D^+ ions is the result of the transition of the molecules H_2 and D_2 into the state $2p\sigma_u$ of the corresponding molecular ion. In the case when the "ion-core" model is applicable, one should expect the group of excited atoms with energy ~ 7 eV to be due to dissociation with transition to a state for which the $2p\sigma_u$ state is the ion core. Such states are known for the H_2 molecule^[19-21] — the doubly excited states of the series $(2p\sigma_u, n/\lambda)$, which converge to the $2p\sigma_u$ state of the molecular ion. Transition from these states via autoionization is possible

either to the ground state of the molecular ion, or to its dissociative continuum. In^[22] it was shown, however, that the states of the series $(2p\sigma_u, n/\lambda)$ can decay also with production of two hydrogen atoms in ground state and excited state. The calculated doubly excited states cross the center of the Franck-Condon region at an energy from 29 to 32 eV. This determines the maximum of the $P(E)$ distribution for the above-described dissociation between 6 and 7 eV for atoms in a state with $n \geq 4$. Another process that leads to the appearance of fast excited hydrogen atom may be the transition of the molecule into the $(2p\sigma_u)^2$ state followed by a transition (at large internuclear distances) from this state into Rydberg states with formation of two atoms as the dissociation products, one in the ground and the other in an excited state. This process was observed in^[11] and led to the appearance of highly excited hydrogen atoms with energy ~ 6 eV in the maximum of the distribution. The $P(E)$ distribution for these atoms at an electron energy 100 eV is shown in Fig. 4b. The maximum of this distribution is shifted towards lower energies compared with the maximum of the distribution for the protons. In our case, in view of the rather large errors in the function $P(E)$, it is difficult to state which of the two described processes plays the principal role in the formation of the fast excited atoms. It must be noted, however, that with increasing principal quantum number the $P(E)$ distribution for the excited atoms shifts towards lower energies, and the relative number of atoms with energy ~ 7 eV decreases appreciably. If this group of excited atoms were the result of the second process, no such decrease would take place. It is thus probable that the main process whereby the group of fast excited atoms with energy ~ 7 eV is produced is dissociation with transition into repulsion states that converge to the $2p\sigma_u$ state of the molecular ion. The reason for the decrease of the relative number of these atoms with increasing n may be the autoionization of the states $(2p\sigma_u, n/\lambda)$, which was proposed in^[23]. According to the model of that reference, these states can decay at large internuclear distances into an H^+ ion and an H^- ion in an excited state. Since the excited H^- ion is unstable, the end products of the dissociation are $H^+ + H + e$. The $P(E)$ distributions shown in Fig. 4 are broader than the $P(E)$ distributions for the ions and highly excited atoms. A group of atoms with energies $< 2-3$ eV is observed in excited hydrogen (deuterium) atoms in states with $n=4, 5$, and 6 . Such atoms can be the result of the dissociation of higher doubly excited states whose decay leads to the appearance of two excited atoms or of an excited atom and an ion.

¹The value of α (the most probable velocity) is taken for a temperature T equal to the gas temperature in the collision chamber.

²To vary the resolving power of the apparatus we varied the distance between the interferometer mirrors. Three mirror-setting variants were used, with spacings 0.3, 0.6 and 3 mm.

³In^[2] the error was determined by returning from the function $P(v)$ in the integration in (3) to the function $\varphi(\lambda)$. The calculated values of $\varphi(\lambda)$ were normally distributed with a set variance, and Eq. (3) was solved anew for these values. The

values of $P(\nu)$ obtained in this manner were compared with the initial ones.

^{4b}The ordinate scales in Figs. 3 and 4 are the same for the H and D atoms. The relative values were chosen such that the total area under the $P(E)$ curve was proportional to the excitation cross sections of the corresponding hydrogen and deuterium lines. The values of the cross section were taken from¹⁰⁾.

^{5b}The symbol n' is used for the principal quantum number of the Rydberg state to distinguish it from the principal quantum number n of the excited dissociation fragments.

¹R. S. Freund, J. A. Schiavone, and D. F. Brader, *J. Chem. Phys.* **64**, 1122 (1976).

²G. N. Polyakova, V. F. Erko, A. I. Ranyuk, and O. S. Pavlichenko, *Zh. Eksp. Teor. Fiz.* **71**, 1755 (1976) [*Sov. Phys. JETP* **44**, 921 (1976)].

³L. Julien, M. Glass-Maujean, and J. P. Descoubes, *J. Phys. B* **6**, L196 (1976).

⁴G. F. Möhlmann, S. Tsurubuchi, and F. J. de Heer, *Chem. Phys.* **18**, 145 (1976).

⁵L. D. Weaver and R. H. Hughes, *J. Chem. Phys.* **52**, 2299 (1970).

⁶R. N. Zare and D. R. Herschbach, *Proc. IEEE* **51**, 173 (1963).

⁷R. N. Zare, *J. Chem. Phys.* **47**, 204 (1967).

⁸G. H. Dunn and L. J. Kieffer, *Phys. Rev.* **132**, 2109 (1963).

⁹R. J. Van Brunt and L. J. Kieffer, *Phys. Rev. A* **2**, 1293 (1970).

¹⁰D. A. Vroom and F. J. de Heer, *J. Chem. Phys.* **50**, 580 (1969).

¹¹J. A. Schiavone, K. C. Smyth, and R. S. Freund, *J. Chem. Phys.* **63**, 1043 (1975).

¹²M. Misakian and J. C. Zorn, *Phys. Rev. A* **6**, 2180 (1972).

¹³P. Borrell, M. Glass-Maujean, and P. M. Guyon, *Abstracts Fourth Intern. Conf. on Vacuum-Ultraviolet Radiat. Phys.*, Hamburg, 1974, p. 30.

¹⁴R. S. Berry and S. E. Nielson, *Phys. Rev. A* **1**, 395 (1970).

¹⁵A. L. Ford and K. K. Docken, *J. Chem. Phys.* **62**, 4955 (1975).

¹⁶R. S. Freund, *J. Chem. Phys.* **54**, 3125 (1971).

¹⁷K. C. Smith, J. A. Schiavone, and R. S. Freund, *J. Chem. Phys.* **59**, 5225 (1973).

¹⁸K. C. Smith, J. A. Schiavone, and R. S. Freund, *J. Chem. Phys.* **60**, 1358 (1974).

¹⁹C. Bottcher and K. Docken, *J. Phys. B* **7**, L5 (1974).

²⁰C. Bottcher, *J. Phys. B* **7**, L352 (1974).

²¹A. U. Hazi, *J. Phys. B* **8**, L262 (1975).

²²A. U. Hazi, *J. Chem. Phys.* **60**, 4358 (1974).

²³A. U. Hazi, *Chem. Phys. Lett.* **25**, 259 (1974).

Translated by J. G. Adashko

Technique of optical polarization measurements of plasma Langmuir turbulence spectrum

A. I. Zhuzhunashvili and E. A. Oks

I. V. Kurchatov Atomic Energy Institute

(Submitted 28 March 1977)

Zh. Eksp. Teor. Fiz. **73**, 2142-2156 (December 1977)

We describe an optical method of measuring the amplitude-angle distribution of a high-frequency Langmuir turbulence; the method is based on a polarization analysis of the Stark profiles of hydrogen spectral lines. We determine with the aid of this method, for the first time ever, both the turbulence level and the directivity pattern of the Langmuir noise produced in a plasma upon annihilation of opposing magnetic fields.

PACS numbers: 52.70.Kz, 52.35.Ra, 52.25.Ps

1. The development of spectroscopic diagnostics based on the Stark effect (see, e.g.,^[1]) has made possible a detailed investigation of the microscopic picture of the turbulent state of a plasma. The performance of such experiments has stimulated a successful development of the theory of Stark broadening of hydrogen and hydrogenlike lines by plasma noise. The theoretical procedure for measuring the level^[2,3] and degree of anisotropy of the directivity pattern^[4] of low-frequency (LF) noise was successfully put into effect in experiments^[5,6]. In the theory of Stark broadening of hydrogen spectral lines by high-frequency (HF) Langmuir noise, the dominant role was played until recently by the adiabatic approximation.^[7,8] The adiabatic theory, however, is not suitable for the calculation of the half-widths of lines having intense central components, such as L_α , H_α , H_γ , and others. For the remaining hydrogen lines, the adiabatic description of the noise action is

suitable only under the following conditions: 1) the spectrum of the HF noise is one-dimensional; 2) the HF noise is polarized along the quasistatic field F ; 3) the plasma has a one-dimensional quasistatic LF noise spectrum with average amplitude $F_0 \gg eN^{2/3}$ (e is the electron charge and N is the plasma concentration).¹⁾

There have been a number of attempts to overcome the limitations in these calculations. Sholin^[2] estimated the Stark-state lifetime determined by the nonadiabatic action of an HF noise spectrum of width $\Delta\Omega \sim \Omega_p$ (Ω_p is the plasma frequency). Kim and Wilhelm^[9] calculated the analytic profile of the simplest hydrogen line L_α under the action of a three-dimensional HF noise spectrum but in the absence of a quasistatic electric field. In other theoretical papers, a computer was used to calculate the action of a static electric field crossed with an HF monochromatic electric field on the splitting